Global long-term passive microwave satellite-based retrievals of vegetation optical depth

Yi Y. Liu,[1,2,3] Richard A. M. de Jeu,[2] Matthew F. McCabe,[1] Jason P. Evans,[4] and Albert I. J. M. van Dijk[3]

Received 26 June 2011; revised 26 August 2011; accepted 29 August 2011; published 22 September 2011.

[1] Vegetation optical depth (VOD) retrievals from three satellite-based passive microwave instruments were merged to produce the first long-term global microwave-based vegetation product. The resulting VOD product spans more than two decades and shows seasonal cycles and inter-annual variations that generally correspond with those observed in the Advanced Very High Resolution Radiometer (AVHRR) Normalized Difference Vegetation Index (NDVI). Some notable differences exist in the long-term trends: the NDVI, operating in the optical regime, is sensitive to chlorophyll abundance and photosynthetically active biomass of the leaves, whereas the microwave-based VOD is an indicator of the vegetation water content in total above-ground biomass, i.e., including wood and leaf components. Preliminary analyses indicate that the fluctuations in VOD typically correlated to precipitation variations, and that the mutually independent VOD and NDVI do not necessarily respond in identical manners. Considering both products together provides a more robust structural characterization and assessment of long-term vegetation dynamics at the global scale. **Citation:** Liu, Y. Y., R. A. M. de Jeu, M. F. McCabe, J. P. Evans, and A. I. J. M. van Dijk (2011), Global long-term passive microwave satellite-based retrievals of vegetation optical depth, *Geophys. Res. Lett.*, *38*, L18402, doi:10.1029/2011GL048684.

1. Introduction

[2] Vegetation dynamics play an important role in the hydrological, energy and carbon cycles, through influences of land cover change on hydrologic responses, interactions with climate and carbon storage and emission [e.g., *D'Odorico et al.*, 2006; *Schimel et al.*, 2001; *Zhang et al.*, 2001]. Satellite observations offer the only means to continuously monitor such variations at the global scale. The Normalized Difference Vegetation Index (NDVI) [*Tucker et al.*, 2005] is probably the most commonly used satellite-based long-term vegetation index, with a time series developed from the Advanced Very High Resolution Radiometer (AVHRR) extending back to 1981. The NDVI is derived by subtracting the red reflectance values from the near-infrared (NIR) and dividing it by the sum of NIR and red bands, i.e., (NIR-red)/(NIR + red). It is a direct measure of radiation absorption by the canopy [*Myneni et al.*, 1995]. Due to leaf structure and chlorophyll content, healthy vegetation absorbs most of the red light and reflects a large portion of the NIR light, resulting in a high value of NDVI. The disadvantages of NDVI are that it is affected by atmospheric influences (e.g., aerosols and cloud) and limited to monitoring the top of the canopy. NDVI eventually saturates at some level of leaf area coverage and cannot detect further changes in leaf reflectance, covarying with leaf biomass.

[3] Unlike optical remote sensing, passive microwave observations can measure both leaf and woody components of aboveground living biomass through a retrieved property termed the vegetation optical depth (VOD) [*Jones et al.*, 2011; *Shi et al.*, 2008], by virtue of the sensitivity of passive microwave emissions to water in the environment. Another advantage is its ability to penetrate cloud cover. The main disadvantage of passive microwave observations is the relatively coarse spatial resolution (>10km) as a result of the low energy of the emissions (the resolution of AVHRR NDVI is <10 km).

[4] There is no consistent continuous satellite-based microwave measurement program that covers a period comparable with AVHRR. However, *Owe et al.* [2008] developed a method to retrieve vegetation information from passive microwave emissions that in principle can be applied to all wavelengths and all sensors. This makes it possible to merge VOD data from different sensors into a long-term time series since 1987. Direct and long-term in-situ measurements of aboveground vegetation dynamics are not available at the scale of satellite measurement. The VOD, like NDVI, is a radiometric parameter rather than a well-defined "easily validated" geophysical parameter. Furthermore, these two vegetation parameters are conceptually different. This prevents any formal validation of a merged long-term VOD product against either in-situ or NDVI data. Instead, the present study analyses the characteristics and interpretation of long-term VOD data through more indirect comparison with global NDVI and precipitation data. Such an approach will highlight consistencies and differences between NDVI and VOD data and identify the potential to use both products to more comprehensively characterize vegetation dynamics.

2. Data and Methods

[5] The VOD retrieval algorithm developed by VU University Amsterdam and NASA (VUA-NASA model) uses a radiative transfer model to extract soil moisture and VOD simultaneously (refer to *Meesters et al.* [2005] and *Owe et al.*

[1]Water Research Centre, School of Civil and Environmental Engineering, University of New South Wales, Sydney, New South Wales, Australia.
[2]Department of Hydrology and Geo-Environmental Sciences, Faculty of Earth and Life Sciences, Vrije Universiteit Amsterdam, Amsterdam, Netherlands.
[3]Black Mountain Laboratories, CSIRO Land and Water, Canberra, ACT, Australia.
[4]Climate Change Research Centre, University of New South Wales, Sydney, New South Wales, Australia.

0094-8276/11/2011GL048684

[2001, 2008] for further details). Essentially, the vegetation is considered to behave like a one-layered semi-transparent medium and the VOD (τ, dimensionless), as a measure of the vegetation transmissivity (Γ) with a negative exponential relationship (see equation (1) in which u is the incidence angle of the observation), represents the degree to which the vegetation attenuates microwave radiation emitted by the underlying soils and the vegetation itself.

$$\Gamma = \exp(-\tau/\cos u) \quad (1)$$

When the VOD equals 0, the corresponding transmissivity is 1, which means that there is no vegetation attenuation on the microwave emission of the soils (i.e., bare soil). The VOD increases with vegetation density; over dense vegetation (e.g., tropical rainforest), the transmissivity gets close to zero and the microwave emissions are dominated by vegetation.

[6] The VOD can be interpreted as being directly proportional to the total vegetation water content, varying with wavelength of the sensor, vegetation structure and viewing angle [*Jackson and Schmugge*, 1991; *Kerr and Njoku*, 1990; *Kirdyashev et al.*, 1979]. In the present study, data from the Special Sensor Microwave Imager (SSM/I, September 1987–2007), TRMM Microwave Imager (TMI, 1998–2008) and Advanced Microwave Scanning Radiometer (AMSR-E, July 2002–2008) were used. Characteristics of these microwave instruments are detailed in Table S1 in the auxiliary material.[1] Only VOD retrievals acquired by night-time overpasses (specified as occurring between 1900 and 0800 local time) are used, as vertical temperature gradients are weaker, and hence more robust retrievals can be obtained [*Owe et al.*, 2008]. Radio Frequency Interference (RFI) on the AMSR-E 6.9GHz retrievals affects the quality of retrievals over United States, Japan and the Middle East [*Njoku et al.*, 2005]. VOD retrievals from 10.7GHz were used over the regions with moderate and strong RFI on 6.9 GHz (see *Li et al.* [2004] for details).

[7] Because of the dependence of sensor characteristics, VOD values vary between instruments. For most of the Earth's land surface, the daily VOD time series from SSM/I, TMI and AMSR-E display strong correlation (Figure S1), which makes it possible to rescale and merge them into a long-term dataset. The mean and range vary between different sensors, which means that a reference dataset needs to be chosen. AMSR-E was selected as this reference, as it has a relatively low measuring frequency which promotes VOD retrieval accuracy, has the highest spatial and temporal resolution, and is still operational. The cumulative distribution frequency (CDF) matching technique was applied to rescale SSM/I and TMI against AMSR-E, after which they were merged into a single continuous time series (see Figure S2 for one example). The rescaling approach does not change the relative dynamics in the original products [see *Liu et al.*, 2011]. More details about the piece-wise linear CDF matching technique are given by *Liu et al.* [2009]. Hereafter the CDF matched product (SSM/I-TMI-AMSR-E) is referred to as the merged VOD product.

[8] The global VOD time series was compared to global time series of NDVI and precipitation. The data sources and pre-processing steps used in the analyses are detailed as follows. For NDVI, the long-term AVHRR based Global Inventory Monitoring and Modeling Studies product (GIMMS, 1981–2006) [*Tucker et al.*, 2005] is used (available from http://glcf.umiacs.umd.edu/data/gimms/). Since VOD retrievals are not available when surface temperature is below 0°, concurrent NDVI data were masked out. To enable spatial and temporal consistency, VOD and NDVI data were resampled to 0.25° and monthly averages. The monthly Global Precipitation Climatology Centre dataset (GPCC, 1901–2009) [*Rudolf et al.*, 2010] (from http://gpcc.dwd.de) was used, along with the University of Maryland (UMD) scheme 14-class MODIS global land cover product [*De Fries et al.*, 1998] (from http://modis-land.gsfc.nasa.gov/landcover.htm and with product code MCD121). The 0.05° resolution data were aggregated to 0.25° resolution using the predominant land cover class.

[9] Spearman's correlation coefficient (r) was calculated for the period 1987–2006 to investigate agreement between monthly averages of VOD and NDVI. The Mann-Kendall trend test [e.g., *Dery and Brown*, 2007; *Lins and Slack*, 1999] was applied to annual averages of VOD and NDVI. Both techniques are non-parametric that are based on relative ranks of sample data rather than absolute values, and do not require any assumptions about the nature of the relationship. Detailed equations regarding these two methods can be obtained from *Helsel and Hirsch* [2002].

3. Results and Discussions

[10] The annual averages of VOD and NDVI during 1987–2006 were calculated for each 0.25° grid cell across the globe and then plotted against each other based on their land cover types (Figure 1). It can be seen that the spatial distribution of VOD and NDVI is highly correlated over grassland and cropland. For forested regions, NDVI is likely to become saturated over dense canopies, whereas VOD may still record differences due primarily to its deeper penetration. Over shrublands, the relationship between VOD and NDVI lies somewhere between grassland, cropland and forest: likely related to the attribute of shrubland as a varying mixture of grass and woody components.

[11] Spatial maps of r between monthly values of VOD and NDVI (Figure 2a) show high correlation over Europe, northeast Asia, India, Australia, Africa, eastern South America and central North America, indicating that VOD generally captures similar seasonal cycles as NDVI. Over tropical regions, the minimal annual variation of VOD leads to lower correlation with NDVI. Over central Russia, the peaks of VOD lag behind NDVI by up to a few months, and agree more closely with precipitation. The reduced correlation over Southeast Asia and arctic Canada may be caused by the VUA-NASA model not accounting for the open surface water variability (e.g., inundation, wetlands, and flood irrigation) which could have a significant spurious impact on retrieved VOD seasonality.

[12] Annual changes in VOD and NDVI during 1987–2006 are shown in Figures 2b and 2c. Both products show similar trends over Alaska, Canadian prairies (Canada-USA), western Russia, the Sahel, India, and northwestern

[1] Auxiliary materials are available in the HTML. doi:10.1029/2011GL048684.

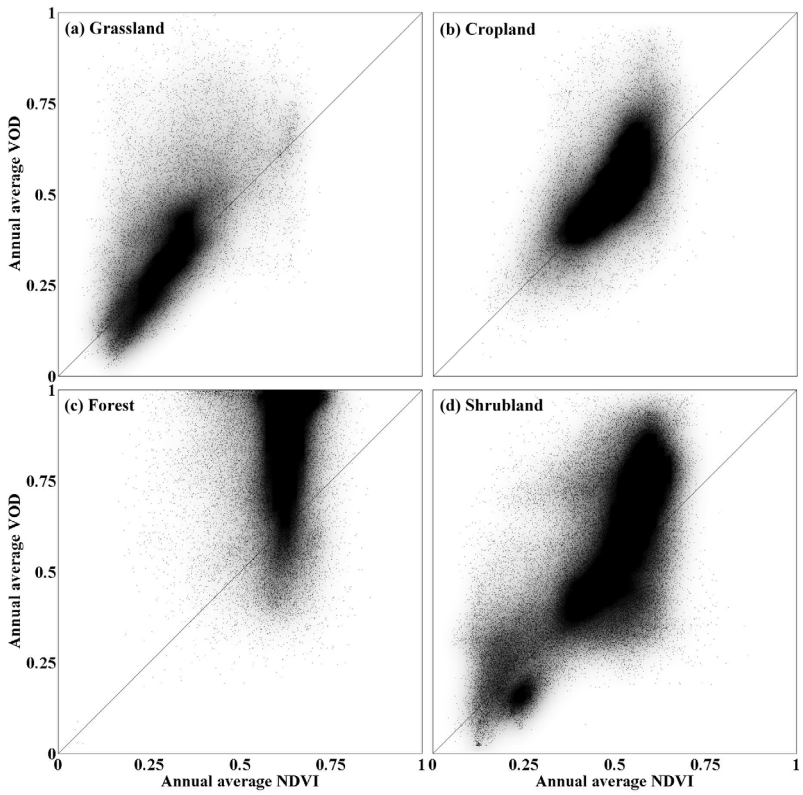

Figure 1. Relationship between annual average NDVI and VOD for 1987–2006 over different land cover types taken for each 0.25° grid cell at the global scale. Here, the forest includes evergreen, deciduous, and mixed forests, while shrubland includes shrubland, woodland and wood/grass. Each scatter plot is overlain by a density plot; black, gray and white, respectively, representing high, medium and low density.

Australia, but dissimilar or even opposite trends over central North America (USA-Mexico), northeast Asia, southern Africa, southeast Australia, Amazon tropical rainforests and southeast Amazon.

[13] To interpret these similarities and differences, annual VOD, NDVI and precipitation were plotted for the regions outlined in Figure 2 (see Figure 3). For regions primarily represented by grassland and shrubland (Figures 3a–3f), the long-term changes in VOD agree well with precipitation, but the trend is sometimes different from that in NDVI. These discrepancies are most likely due to the different vegetation characteristics represented by VOD (water content in both foliage and woody biomass) and NDVI (canopy cover). Thus, the total above-ground biomass (i.e., VOD) of grassland may decline in precipitation, but the NDVI may remain unchanged as long as green canopy cover is maintained. The land cover categories labeled 'shrubland' are a varying mixture of herbaceous and woody plants. If declines in VOD are largely caused by declines in the woody biomass component, this may be associated with an increase in the herbaceous vegetation cover and hence NDVI may not decline; and vice versa.

[14] Over cropland regions (Figures 3g–3i), both VOD and NDVI show long-term increases even where precipitation does not. It seems reasonable to assume that the agricultural intensification for these regions reported by the Food and Agriculture Organization (see statistics on http://faostat.fao.org) might also be associated with an increase in (mean) canopy cover and total biomass.

[15] Over the boreal forests of Alaska (Figure 3j) both vegetation products show similar fluctuations and decreasing trends. Over the Amazon rainforests (Figure 3k), VOD values are high with little inter-annual variations, whereas NDVI values increase slightly. However, this seems primarily due to the anomalously low NDVI values in 1991 and 1994. Following *Kobayashi and Dye* [2005], we attribute these low values to aerosol contamination from the eruption of Mount Pinatubo in 1991 and biomass burning. The southeast Amazon region (Figure 3l) is a known hotspot of large-scale deforestation [*Achard et al.*, 2002; *Hansen et al.*, 2008], which is evident in the microwave-based VOD time series, but not in the NDVI time series. This seems related to the influences of aerosol contamination on NDVI as well.

4. Conclusions

[16] A microwave-based global vegetation product (VOD) of more than 20 years was developed and compared with an existing AVHRR NDVI product. The results reveal that the VOD product captures similar seasonal cycles and inter-annual variations as NDVI over most regions. As expected from its theoretical basis, inter-annual variations in VOD in many (water-limited) regions correspond to varia-

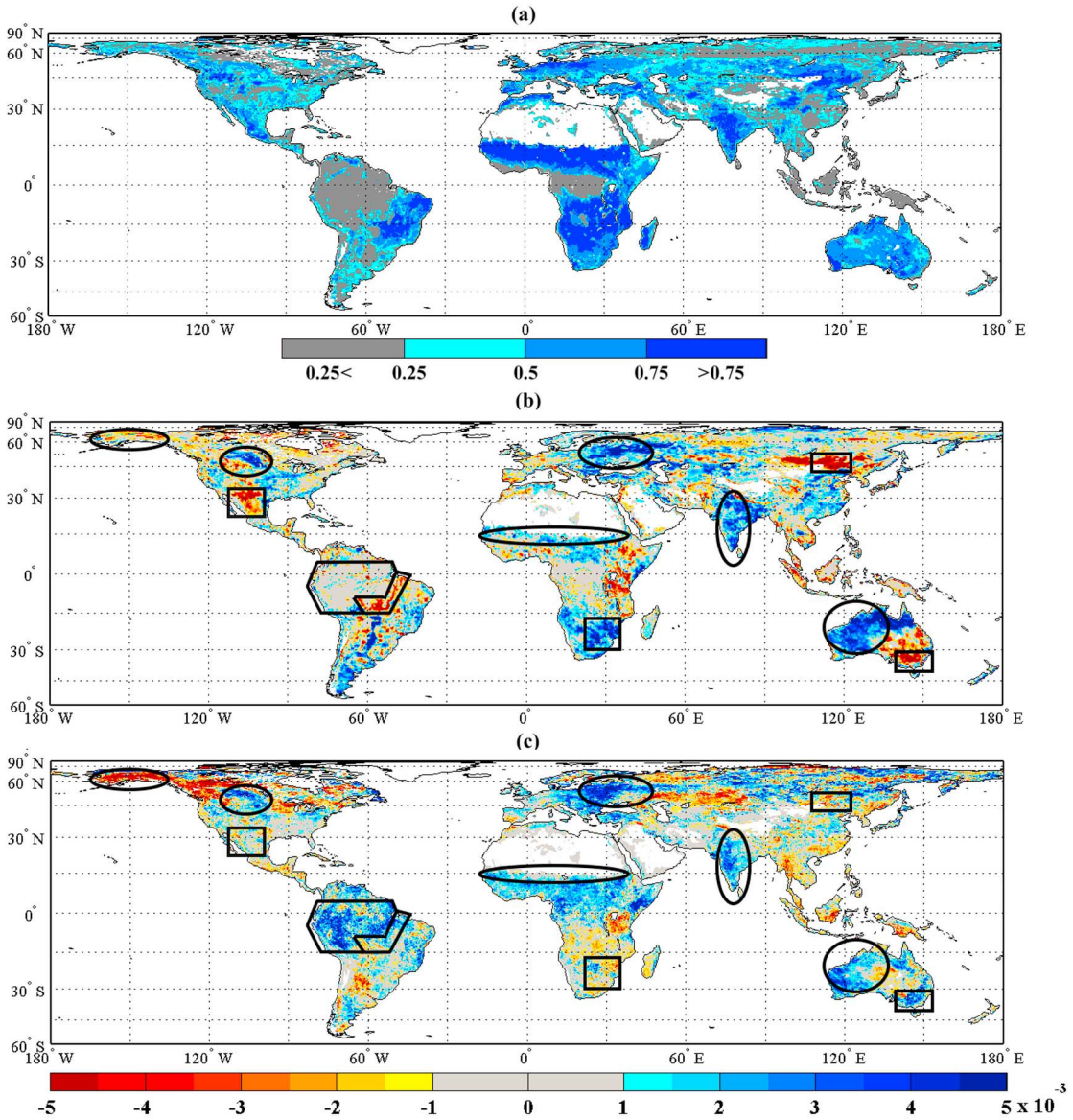

Figure 2. (a) Correlation coefficient (r) between monthly VOD and NDVI for 1987 through 2006; and trends in annual averages of (b) VOD and (c) NDVI from 1988 through 2006 (unit: change per year). The ranges of annual averages of VOD and NDVI (see Figure 1) are 0 to 1 and 0.1 to 0.8, respectively.

tions in precipitation. While NDVI is rapidly saturated for vegetation with a near-closed canopy, the VOD continues to distinguish structural differences. More importantly, the VOD product provides unique global information about long-term vegetation changes over ecosystems with a mixture of herbaceous and woody vegetation components, and appears to detect large-scale deforestation over tropical regions better than NDVI, due to its greater penetration ability.

[17] Nevertheless, this VOD product has its limitations. Several assumptions are made in the current VUA-NASA model, including: a constant single scattering albedo, canopy surface temperature equal to soil surface temperature, equality of vegetation parameters for both horizontal and vertical polarizations, and a fixed surface roughness value [*Owe et al.*, 2001]. The influences of these assumptions on VOD retrieval accuracy and possible improvements of the current model require further focused investigations. In addition, the CDF matching and merging of VOD retrievals from different sensors combine all of these assumptions together with differences in sensor calibration, center frequencies, bandwidth and other sensor specific features. Likewise, the GIMMS NDVI product also suffers similar problems, with sensor inter-calibration, atmospheric corrections, sensor drift all affecting data integrity. These uncertainties inherent in both vegetation products underscore the importance of employing mutually independent products for vegetation studies. Such an approach is expected to yield more comprehensive information from which to characterize vegetation structure, spatial patterns and behaviour, and detect of long-term trends and dynamics at the global scale for multi-disciplinary investigation.

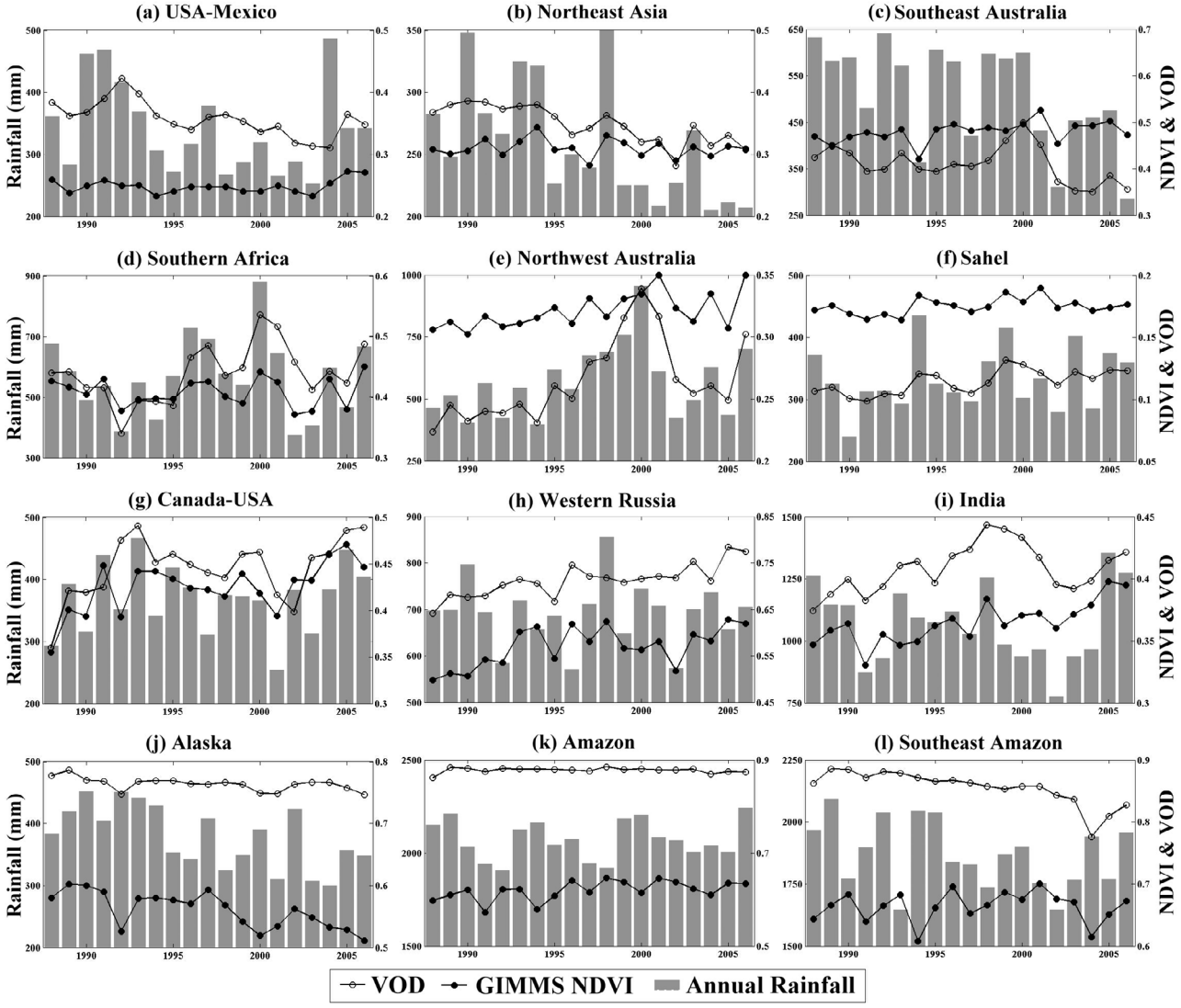

Figure 3. Annual average VOD, NDVI and total precipitation from 1988 through 2006 for the twelve regions outlined in Figure 2. Both VOD and NDVI are presented in their original values and share the right-hand y-axis. Note that vertical scales vary for visualization purpose.

[18] **Acknowledgments.** This work was supported by a University of New South Wales University International Postgraduate Award (UIPA) and a scholarship from the CSIRO Water for a Healthy Country Flagship Program. We would like to thank the anonymous reviewers for their thoughtful comments on an earlier version of the paper.

[19] The Editor thanks an anonymous reviewer for their assistance in evaluating this paper.

References

Achard, F., H. D. Eva, H. J. Stibig, P. Mayaux, J. Gallego, T. Richards, and J. P. Malingreau (2002), Determination of deforestation rates of the world's humid tropical forests, *Science*, *297*(5583), 999–1002, doi:10.1126/science.1070656.

De Fries, R. S., M. Hansen, J. R. G. Townshend, and R. Sohlberg (1998), Global land cover classifications at 8 km spatial resolution: The use of training data derived from Landsat imagery in decision tree classifiers, *Int. J. Remote Sens.*, *19*(16), 3141–3168, doi:10.1080/014311698214235.

Dery, S. J., and R. D. Brown (2007), Recent Northern Hemisphere snow cover extent trends and implications for the snow-albedo feedback, *Geophys. Res. Lett.*, *34*, L22504, doi:10.1029/2007GL031474.

D'Odorico, P., F. Laio, and L. Ridolfi (2006), Vegetation patterns induced by random climate fluctuations, *Geophys. Res. Lett.*, *33*, L19404, doi:10.1029/2006GL027499.

Hansen, M. C., et al. (2008), Humid tropical forest clearing from 2000 to 2005 quantified by using multitemporal and multiresolution remotely sensed data, *Proc. Natl. Acad. Sci. U. S. A.*, *105*(27), 9439–9444, doi:10.1073/pnas.0804042105.

Helsel, D. R., and R. M. Hirsch (2002), Statistical methods in water resources, in *Hydrologic Analysis and Interpretation*, *U.S. Geol. Surv. Tech. Water Resour. Invest.*, *Book 4, Chap. A3*, 510 pp.

Jackson, T. J., and T. J. Schmugge (1991), Vegetation effects on the microwave emission of soils, *Remote Sens. Environ.*, *36*(3), 203–212, doi:10.1016/0034-4257(91)90057-D.

Jones, M. O., L. A. Jones, J. S. Kimball, and K. C. McDonald (2011), Satellite passive microwave remote sensing for monitoring global land surface phenology, *Remote Sens. Environ.*, *115*(4), 1102–1114, doi:10.1016/j.rse.2010.12.015.

Kerr, Y. H., and E. G. Njoku (1990), A semiempirical model for interpreting microwave emission from semiarid land surfaces as seen from space, *IEEE Trans. Geosci. Remote Sens.*, *28*(3), 384–393, doi:10.1109/36.54364.

Kirdyashev, K. P., A. A. Chukhlantsev, and A. M. Shutko (1979), Microwave radiation of the Earth's surface in the presence of a vegetation cover, *Radio Eng. Electron. Phys., Engl. Transl.*, *24*(2), 37–44.

Kobayashi, H., and D. G. Dye (2005), Atmospheric conditions for monitoring the long-term vegetation dynamics in the Amazon using normalized

difference vegetation index, *Remote Sens. Environ.*, *97*(4), 519–525, doi:10.1016/j.rse.2005.06.007.

Li, L., E. G. Njoku, E. Im, P. S. Chang, and K. S. Germain (2004), A preliminary survey of radio-frequency interference over the US in Aqua AMSR-E data, *IEEE Trans. Geosci. Remote Sens.*, *42*(2), 380–390, doi:10.1109/TGRS.2003.817195.

Lins, H. F., and J. R. Slack (1999), Streamflow trends in the United States, *Geophys. Res. Lett.*, *26*(2), 227–230, doi:10.1029/1998GL900291.

Liu, Y. Y., A. I. J. M. van Dijk, R. A. M. de Jeu, and T. R. H. Holmes (2009), An analysis of spatiotemporal variations of soil and vegetation moisture from a 29-year satellite-derived data set over mainland Australia, *Water Resour. Res.*, *45*, W07405, doi:10.1029/2008WR007187.

Liu, Y. Y., R. M. Parinussa, W. A. Dorigo, R. A. M. de Jeu, W. Wagner, A. I. J. M. van Dijk, M. F. McCabe, and J. P. Evans (2011), Developing an improved soil moisture dataset by blending passive and active microwave satellite-based retrievals, *Hydrol. Earth Syst. Sci.*, *15*(2), 425–436, doi:10.5194/hess-15-425-2011.

Meesters, A. G. C. A., R. A. M. de Jeu, and M. Owe (2005), Analytical derivation of the vegetation optical depth from the microwave polarization difference index, *IEEE Geosci. Remote Sens. Lett.*, *2*(2), 121–123, doi:10.1109/LGRS.2005.843983.

Myneni, R. B., F. G. Hall, P. J. Sellers, and A. L. Marshak (1995), The interpretation of spectral vegetation indexes, *IEEE Trans. Geosci. Remote Sens.*, *33*(2), 481–486, doi:10.1109/36.377948.

Njoku, E. G., P. Ashcroft, T. K. Chan, and L. Li (2005), Global survey and statistics of radio-frequency interference in AMSR-E land observations, *IEEE Trans. Geosci. Remote Sens.*, *43*(5), 938–947, doi:10.1109/TGRS.2004.837507.

Owe, M., R. de Jeu, and J. Walker (2001), A methodology for surface soil moisture and vegetation optical depth retrieval using the microwave polarization difference index, *IEEE Trans. Geosci. Remote Sens.*, *39*(8), 1643–1654, doi:10.1109/36.942542.

Owe, M., R. de Jeu, and T. Holmes (2008), Multisensor historical climatology of satellite-derived global land surface moisture, *J. Geophys. Res.*, *113*, F01002, doi:10.1029/2007JF000769.

Rudolf, B., A. Becker, U. Schneider, A. Meyer-Christoffer, and M. Ziese (2010), GPCC full data reanalysis version 5, Global Precip. Climatol. Cent., Offenbach, Germany.

Schimel, D. S., et al. (2001), Recent patterns and mechanisms of carbon exchange by terrestrial ecosystems, *Nature*, *414*, 169–172, doi:10.1038/35102500.

Shi, J. C., T. Jackson, J. Tao, J. Du, R. Bindlish, L. Lu, and K. S. Chen (2008), Microwave vegetation indices for short vegetation covers from satellite passive microwave sensor AMSR-E, *Remote Sens. Environ.*, *112*(12), 4285–4300, doi:10.1016/j.rse.2008.07.015.

Tucker, C. J., J. E. Pinzon, M. E. Brown, D. A. Slayback, E. W. Pak, R. Mahoney, E. F. Vermote, and N. El Saleous (2005), An extended AVHRR 8-km NDVI dataset compatible with MODIS and SPOT vegetation NDVI data, *Int. J. Remote Sens.*, *26*(20), 4485–4498, doi:10.1080/01431160500168686.

Zhang, L., W. Dawes, and G. Walker (2001), Response of mean annual evapotranspiration to vegetation changes at catchment scale, *Water Resour. Res.*, *37*(3), 701–708, doi:10.1029/2000WR900325.

R. A. M. de Jeu, Department of Hydrology and Geo-Environmental Sciences, Faculty of Earth and Life Sciences, Vrije Universiteit Amsterdam, De Boelelaan 1085-1087, NL-1081 HV Amsterdam, Netherlands.

J. P. Evans, Climate Change Research Centre, University of New South Wales, Sydney, NSW 2052, Australia.

A. I. J. M. van Dijk, Black Mountain Laboratories, CSIRO Land and Water, GPO Box 1666, Canberra, ACT 2601, Australia. (yi.y.liu@csiro.au)

Y. Liu and M. F. McCabe, Water Research Centre, School of Civil and Environmental Engineering, University of New South Wales, Sydney, NSW 2052, Australia.